Supporting Information

Facet-dependent CO_2 Reduction Reactions on the Kesterite Cu_2ZnSnS_4 Photo-electro Integrated Electrodes

Ruifen Zhang,[a] Xin Wen,*[a] Hongliang Peng,[a] Yongpeng Xia,[a] Fen Xu[a] and Lixian Sun*[a]

[a] Guangxi Key Laboratory of Information Materials, Guangxi Collaborative Innovation Center of Structure and Property for New Energy and Materials, School of Material Science and Engineering, Guilin University of Electronic Technology, Guilin 541004, China
*E-mail: wenxin@guet.edu.cn (X. Wen), sunlx@guet.edu.cn (L. Sun)

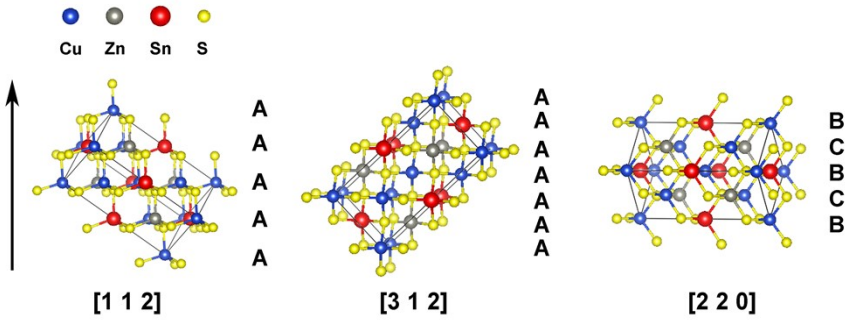

Figure S1. Illustration of [1 1 2], [3 1 2] and [2 2 0] crystal orientations for the kesterite CZTS structure. For [1 1 2] and [3 1 2], there is only one type of plane (A), which includes all metal elements. For [2 2 0], there are two types of plane (B and C), which includes the metal elements of Cu,Sn (B) and Cu,Zn (C), respectively.

	Surface Energy (J/m^2)
(112)	0.156
(220)-CuZn	0.349
(220)-CuSn	0.671
(312)	0.592

Table S1. Surface energies of different facets.

		Cu1	Cu2	Zn	Sn	S1	S2	S3	S4
Top layer	(112)	+0.44	+0.41	+0.83	+0.88	-0.84	-0.84	-0.87	-0.77
	(220)-CuZn		+0.47	+0.82		-0.73	-0.74		
	(220)-CuSn		+0.47		+0.99	-0.75	-0.72		
	(312)	+0.48	+0.45	+0.82	+1.01	-0.78	-0.67	-0.35	-0.41
2nd layer	(112)	+0.49	+0.46	+0.84	+1.31	-0.74	-0.76	-0.74	-0.75
	(220)-CuZn	+0.50			+1.32			-0.74	-0.75
	(220)-CuSn	+0.49		+0.85				-0.76	-0.71

	(312)	+0.50	+0.50	+0.86	+1.32	-0.76	-0.78	-0.73	-0.75
Bulk		+0.52	+0.47	+0.82	+1.31	-0.78	-0.78	-0.78	-0.78

Table S2. The atom's net charge calculated by the Bader charge analysis. (Net charge = Valence charge - Total Bader charge, Charge Unit (|e|), the valence charges of Cu, Zn, Sn and S are 11, 12, 4 and 6, respectively.)

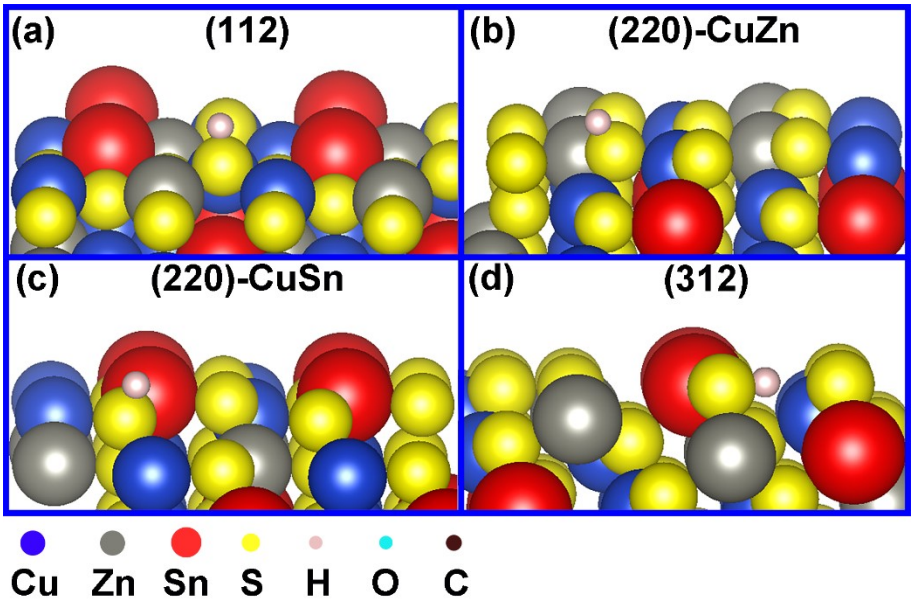

Figure S2. The most stable intermediate structure of *H on (a) (112), (b) (220)-CuZn, (c) (220)-CuSn and (d) (312).

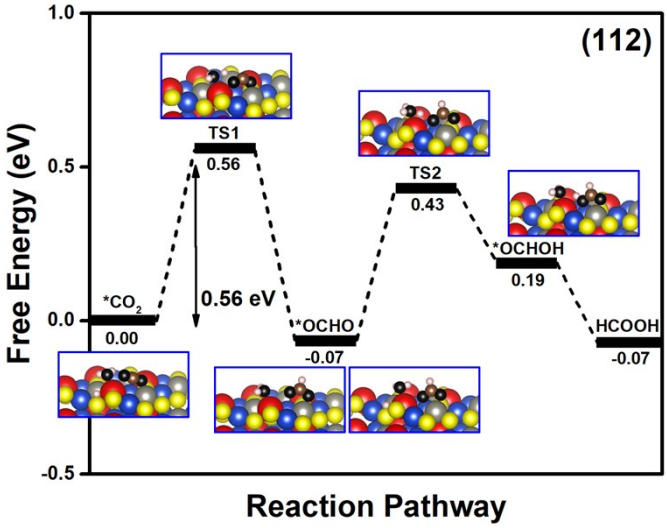

Figure S3. The free energy profiles for formic acid production on (112) facet. The optimized structures of initial states, transition states (TS) and final states are shown in the insets. Blue, gray, red, yellow, black, brown and light brown spheres represent Cu, Zn, Sn, S, O, C and H atoms, respectively.

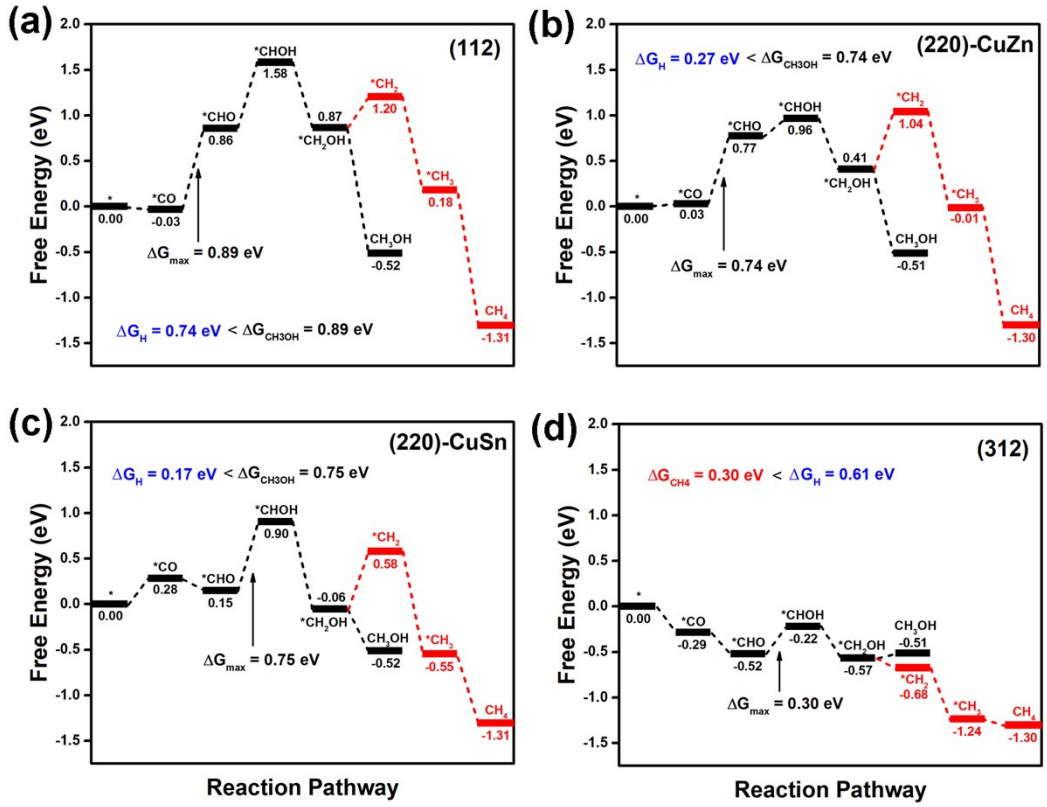

Figure S4. The CORR profiles on (a) (112), (b) (220)-CuZn, (c) (220)-CuSn and (d) (312) with one water molecule in the model.

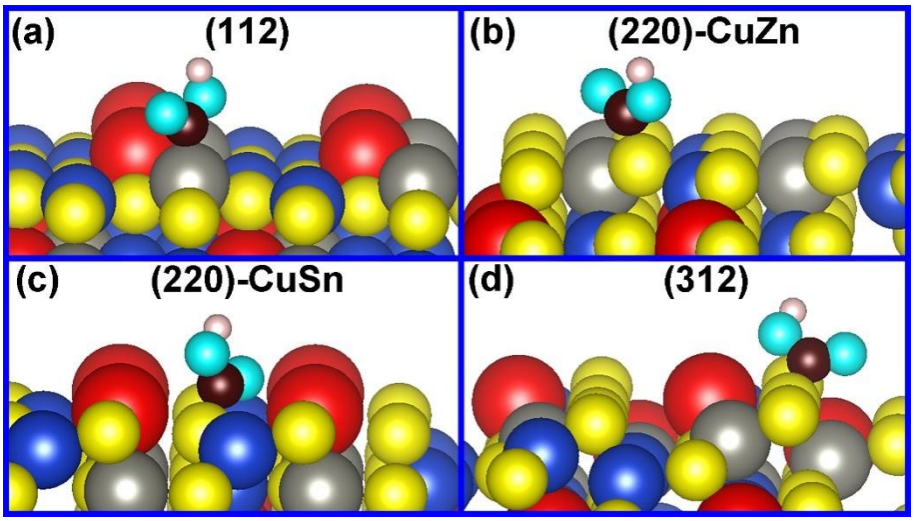

Figure S5. The most stable intermediate structure of *COOH on (a) (112), (b) (220)-CuZn, (c) (220)-CuSn and (d) (312).

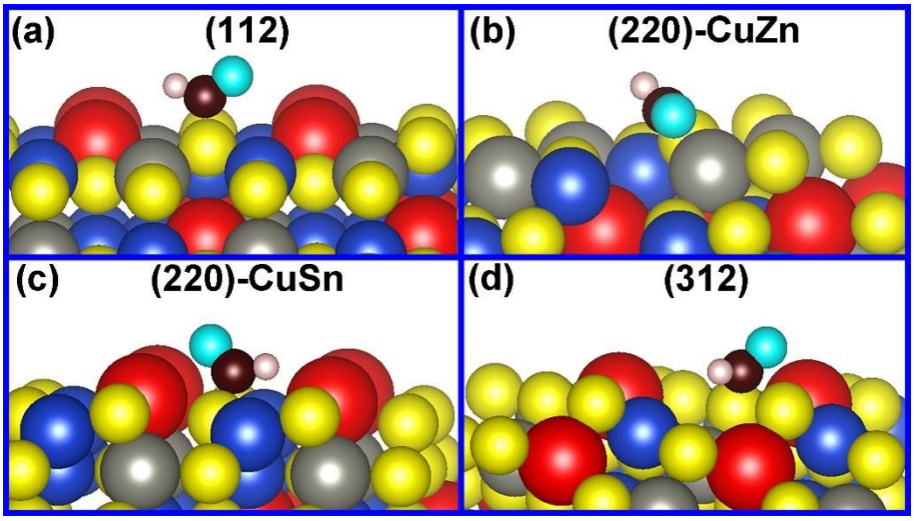

Figure S6. The most stable intermediate structure of *CHO on (a) (112), (b) (220)-CuZn, (c) (220)-CuSn and (d) (312).

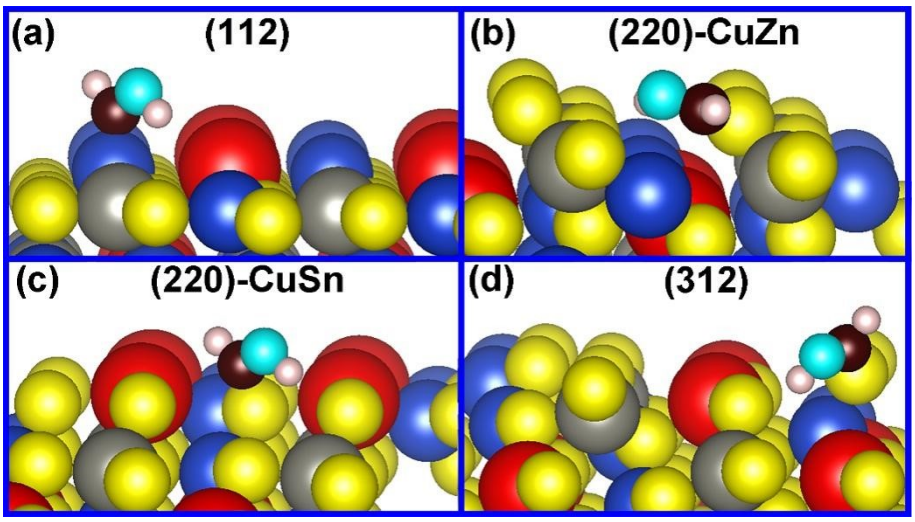

Figure S7. The most stable intermediate structure of *CHOH on (a) (112), (b) (220)-CuZn, (c) (220)-CuSn and (d) (312).

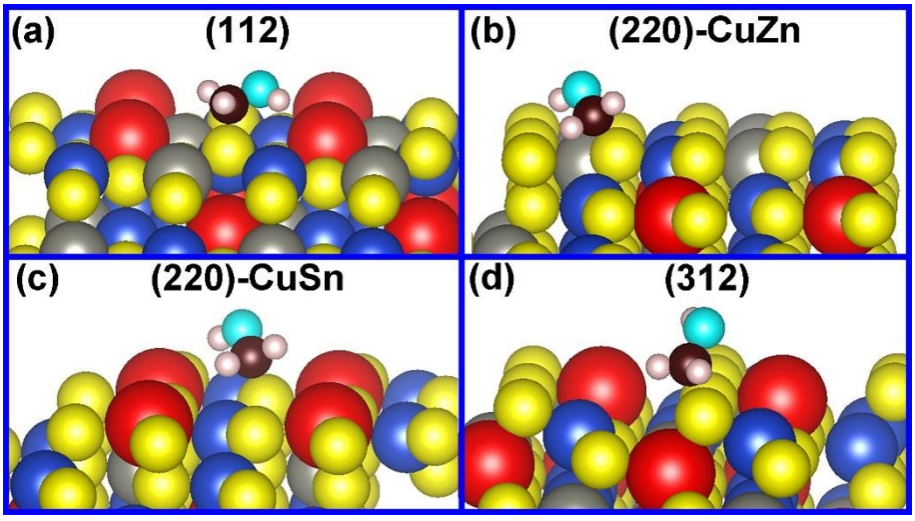

Figure S8. The most stable intermediate structure of *CH_2OH on (a) (112), (b) (220)-CuZn, (c) (220)-CuSn and (d) (312).

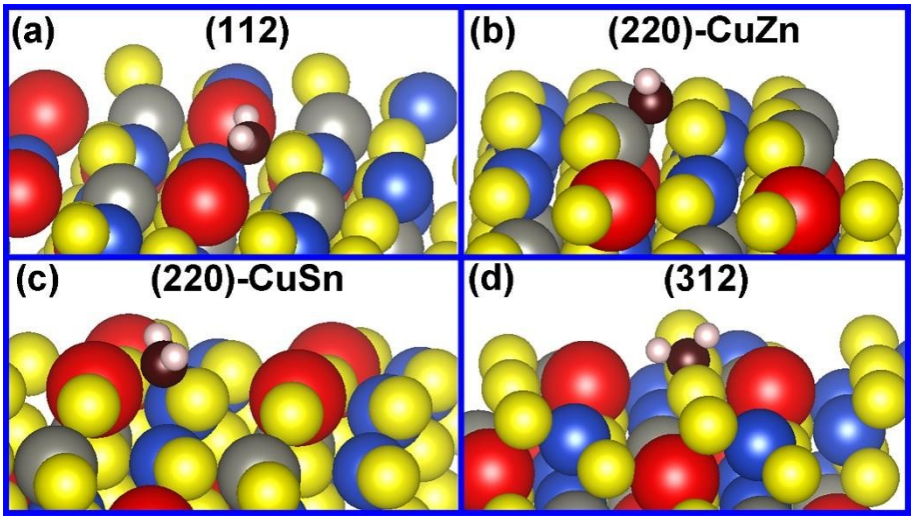

Figure S9. The most stable intermediate structure of *CH_2 on (a) (112), (b) (220)-CuZn, (c) (220)-CuSn and (d) (312).

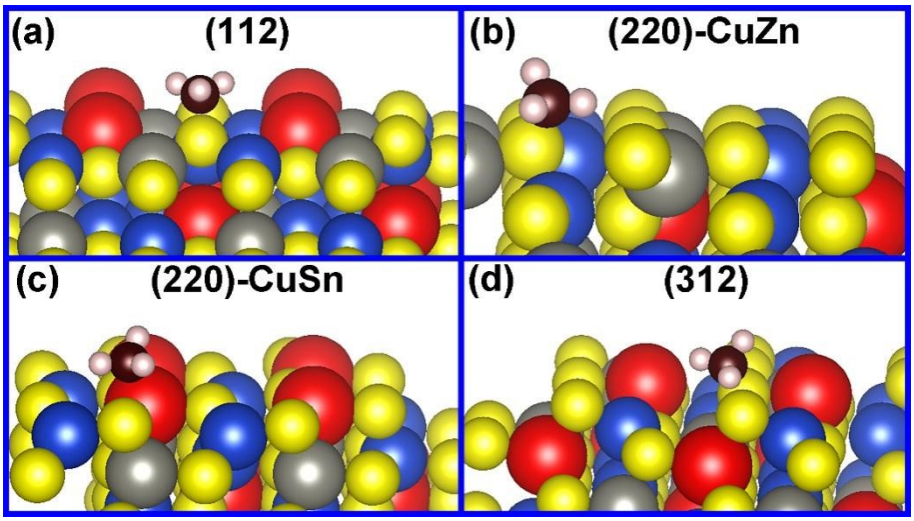

Figure S10. The most stable intermediate structure of *CH_3 on (a) (112), (b) (220)-CuZn, (c) (220)-CuSn and (d) (312).

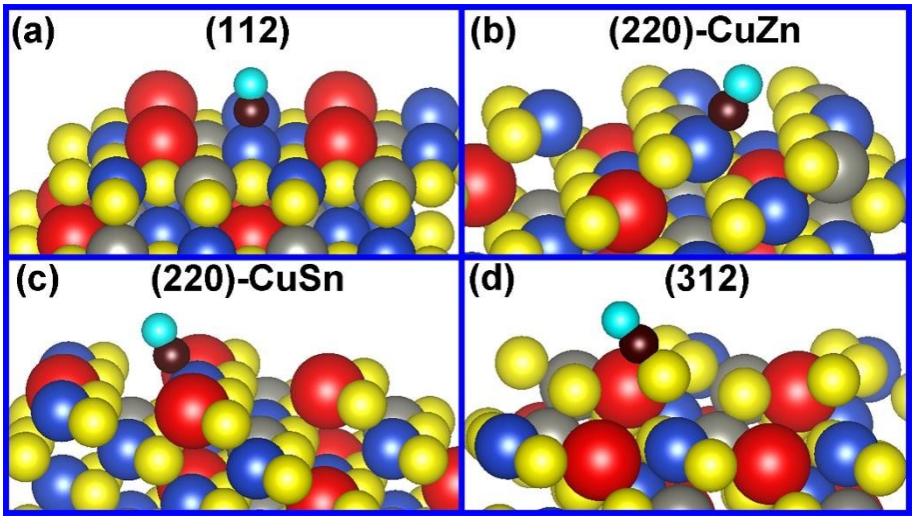

Figure S11. The most stable intermediate structure of *CO on (a) (112), (b) (220)-CuZn, (c) (220)-CuSn and (d) (312).

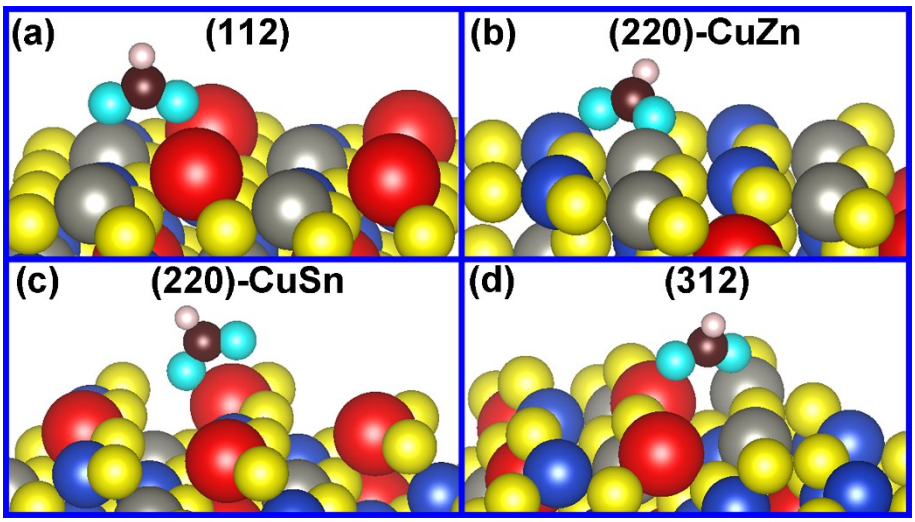

Figure S12. The most stable intermediate structure of *OCHO on (a) (112), (b) (220)-CuZn, (c) (220)-CuSn and (d) (312).

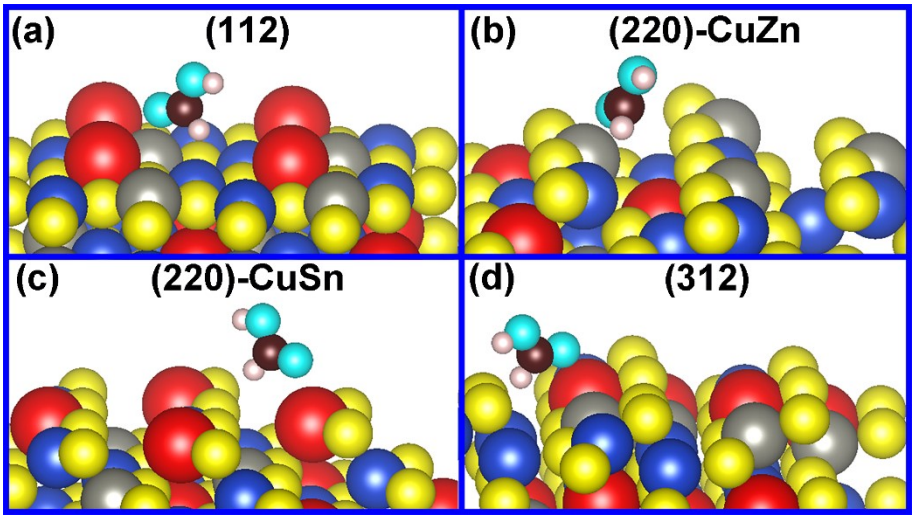

Figure S13. The most stable intermediate structure of *OCHOH on (a) (112), (b) (220)-CuZn, (c) (220)-CuSn and (d) (312).

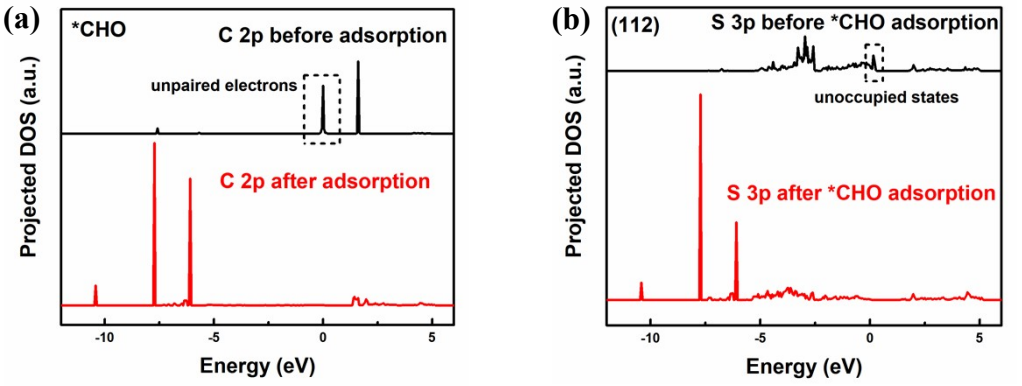

Figure S14. (a) PDOS of C 2p orbital in *CHO before and after adsorption on (112) surface. (b) PDOS of S 3p orbital corresponding to the adsorption-site S atom on (112) surface before and after adsorption of *CHO. Both PDOS were calculated with PBE method.